Contribution from the Departments of Chemistry, Faculty of Pharmacy and Biochemistry, University of Zagreb, 41001 Zagreb, Croatia, Yugoslavia, and New Mexico State University, Las Cruces, New Mexico 88003

Kinetics of Stepwise Hydrolysis of Ferrioxamine B and of Formation of Diferrioxamine B in Acid Perchlorate Solution

Mladen Biruš,[1] Zdravko Bradić,[2] Gordana Krznarić,[1] Nikola Kujundžic,[1] Marijan Pribanić,*[1] Patricia C. Wilkins,[2] and Ralph G. Wilkins*[2]

Received July 2, 1986

Kinetic and thermodynamic parameters for the hydrolysis of ferrioxamine B, $Fe(HDFB)^+ + 3H^+ \rightleftarrows Fe^{3+} + H_4DFB^+$, in 0.005–1.0 M acid at 25 °C and ionic strength 2.0 M ($NaClO_4/HClO_4$) have been obtained by stopped-flow and rapid-scan spectral methods. Four stages can be separated. These consist of (a) $Fe(HDFB)^+ + H^+ \rightleftarrows Fe(H_2DFB)^{2+}$, (b) transformation of $Fe(H_2DFB)^{2+}$ to another form $Fe(H_2DFB)^{2+*}$ without H^+ change, (c) $Fe(H_2DFB)^{2+*} + H^+ \rightleftarrows Fe(H_3DFB)^{3+}$, and (d) $Fe(H_3DFB)^{3+} + H^+ \rightleftarrows Fe^{3+} + H_4DFB^+$. The equilibrium constants for each stage were determined by rapid-scan spectral methods and the rate laws by stopped-flow methods. The kinetics of stage d were checked by examining the reverse direction. Agreement between equilibrium constants determined by spectral means and from the kinetics was fair to good. The results were compared with those of previous investigators. The kinetics of formation and decomposition of the binuclear complex $Fe_2(HDFB)^{4+}$ from Fe^{3+} and $Fe(HDFB)^+$ were also determined at 25 °C and ionic strength 2.0 M ($NaClO_4/HClO_4$). A relationship between the hydrolysis and the formation of the dimer was shown.

Siderophore chemistry is a very popular area for research in view of its importance for understanding microbial iron transport.[3-6] One of the most extensively studied siderophore complexes is ferrioxamine B ($(FeHDFB)^+$, **1**) because of its important role

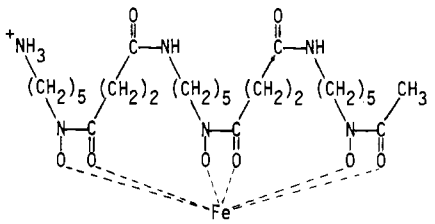

1

in iron bioavailability and chelation therapy. In addition, ferrioxamine B is an interesting chelate complex, the study of which from a purely inorganic chemistry viewpoint will enhance our understanding of the detailed mechanisms by which chelates unravel and form.[7]

A number of studies of the formation and hydrolysis[8-14] as well as ligand-interchange reactions[15,16] of ferrioxamine B in aqueous acid have been reported. There are some differences in the results obtained, particularly with respect to the number of stages discerned in the hydrolysis of ferrioxamine B in acid solution. In this paper we present the results of a detailed examination of the equilibria and kinetic aspects of the hydrolysis of ferrioxamine B in acid solution. We have used perchlorate ion to adjust ionic strength to avoid complications due to iron(III)–anion complexing. Data for the formation of ferrioxamine B are also included, and our results both augment and correct previous studies of the system.[11,13] In addition, the kinetics of formation of the binuclear complex, diferrioxamine B, proposed structure **2**, from ferrioxamine B and iron(III) studied in chloride medium,[12,14,17,18] have been reinvestigated in perchlorate. The hydrolysis and dimer formation are intimately related. Rapid-scan stopped-flow methods have been invaluable in the prosecution of this work.[19]

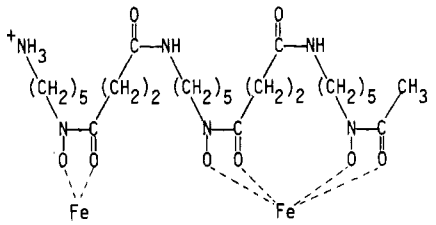

2

Experimental Section

Reagents were chemically pure. The methanesulfonate salt of desferrioxamine B (Desferal) was kindly supplied by the Ciba-Geigy Corp. The salt was recrystallized from methanol and was stored in a vacuum desiccator over P_4O_{10} (mp 149–151 °C). Ferrioxamine B perchlorate was prepared according to a literature procedure.[11] Stock solutions of iron(III) in perchloric acid were prepared from $Fe(ClO_4)_3 \cdot 6H_2O$ (Merck) and standardized by using a molar extinction coefficient of 4.16×10^3 M^{-1} cm^{-1} at 240 nm.[20] Perchloric acid solutions were obtained by dilution of 70% perchloric acid, and sodium perchlorate solutions were prepared from anhydrous sodium perchlorate (G. F. Smith). All solutions were prepared from doubly distilled water from alkaline $KMnO_4$ in an all-glass apparatus.

For the experiments designed to determine the equilibria constants of the various stages of the hydrolysis, $Fe(HDFB)^+$ (0.27 mM) at pH ~6 and ionic strength 2 M ($NaClO_4$) was mixed with $HClO_4$ (0.04–2.0 M) at ionic strength 2 M in a Harrick rapid-scan monochromator linked with a Dionex stopped-flow apparatus, the whole interfaced with an OLIS data collecting system (On Line Instrument Systems, Jefferson, GA). The spectra were run at the completion of each stage, and the absorbances at several wavelengths were tabulated. Most of the analyses were at 426 nm. The kinetic experiments used an OLIS–Dionex stopped-flow

(1) University of Zagreb.
(2) New Mexico State University.
(3) Raymond, K. N.; Tufano, T. P. In *The Biological Chemistry of Iron*; Dunford, H. B., Dolphin, D., Raymond, K. N., Sieker, L., Eds.; Reidel: Dordrecht, Holland, 1982; p 85. (b) Nielands, J. B. *Adv. Inorg. Biochem.* **1983**, *5*, Chapter 6.
(4) Raymond, K. N.; Müller, G.; Matzanke, B. F. *Top. Curr. Chem.* **1984**, *123*, 49.
(5) Nielands, J. B. *Struct. Bonding (Berlin)* **1984**, *58*, 1. Hider, R. C. *Struct. Bonding (Berlin)* **1984**, *58*, 25.
(6) Kehl, H., Ed. *Chemistry and Biology of Hydroxamic Acids*; Karger: New York, 1982.
(7) Margerum, D. W.; Cayley, G. R.; Weatherburn, D. C.; Pagenkopf, G. K. In *Coordination Chemistry*; Martell, A. E., Ed.; American Chemical Society: Washington, DC, 1978; p 1. Wilkins, R. G. *Comments Inorg. Chem.* **1983**, *2*, 187.
(8) Schwarzenbach, G.; Schwarzenbach, K. *Helv. Chim. Acta* **1963**, *46*, 1390.
(9) Lentz, D. J.; Henderson, G. H.; Eyring, E. M. *Mol. Pharmacol.* **1973**, *6*, 514.
(10) Kazmi, S. A.; McArdle, J. V. *J. Inorg. Biochem.* **1981**, *15*, 153.
(11) Monzyk, B.; Crumbliss, A. L. *Inorg. Chim. Acta* **1981**, *55*, L5; *J. Am. Chem. Soc.* **1982**, *104*, 4921.
(12) Biruš, M.; Bradić, Z.; Kujundžić, N.; Pribanić, M. *Inorg. Chim. Acta* **1981**, *56*, L43.
(13) Biruš, M.; Bradić, Z.; Kujundžić, N.; Pribanić, M. *Croat. Chem. Acta* **1983**, *56*, 61.
(14) Biruš, M.; Bradić, Z.; Kujundžić, N.; Pribanić, M. *Inorg. Chem.* **1984**, *23*, 2170.
(15) Tufano, T. P.; Raymond, K. N. *J. Am. Chem. Soc.* **1981**, *103*, 6617.
(16) Monzyk, B.; Crumbliss, A. L. *J. Inorg. Biochem.* **1983**, *19*, 19.
(17) Biruš, M.; Bradić, Z.; Kujundžić, N.; Pribanić, M. *Acta Pharm. Jugosl.* **1983**, *32*, 163.
(18) Biruš, M.; Bradić, Z.; Kujundžić, N.; Pribanić, M. *Inorg. Chim. Acta* **1983**, *78*, 87. Strong, but not overwhelming, evidence is given for the formulation of the dimer as **2** rather than as the more symmetrical form in which each Fe is 3-coordinated to the ligand.
(19) Biruš, M.; Bradić, Z.; Kujundžić, N.; Pribanić, M.; Wilkins, P. C.; Wilkins, R. G. *Inorg. Chem.* **1985**, *24*, 3980.
(20) Bastian, R.; Weberling, R.; Palilla, F. *Anal. Chem.* **1956**, *28*, 459.

0020-1669/87/1326-1000$01.50/0

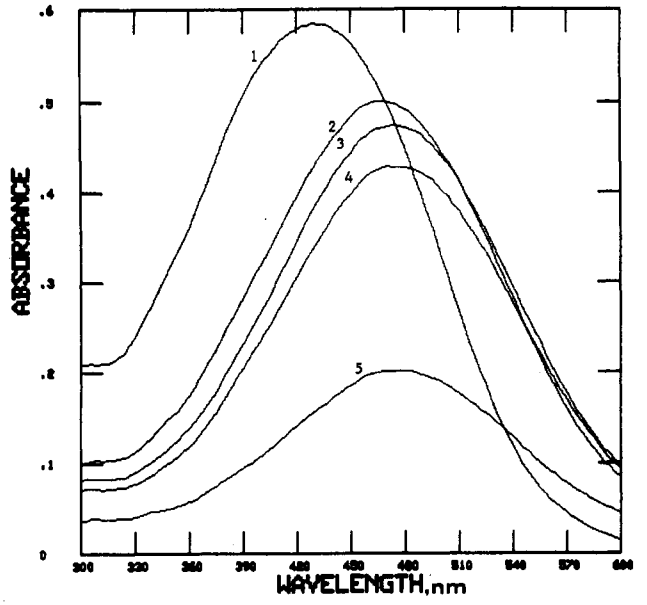

Figure 1. Spectra at the end of each of four stages of hydrolysis of 136 μM ferrioxamine B in 1.0 M $HClO_4$ (I = 2.0 M ($NaClO_4$); optical path length 1.72 cm): curve 1, reactant spectrum, pH 6; curves 2–5, spectra at end of stages I–IV, respectively.

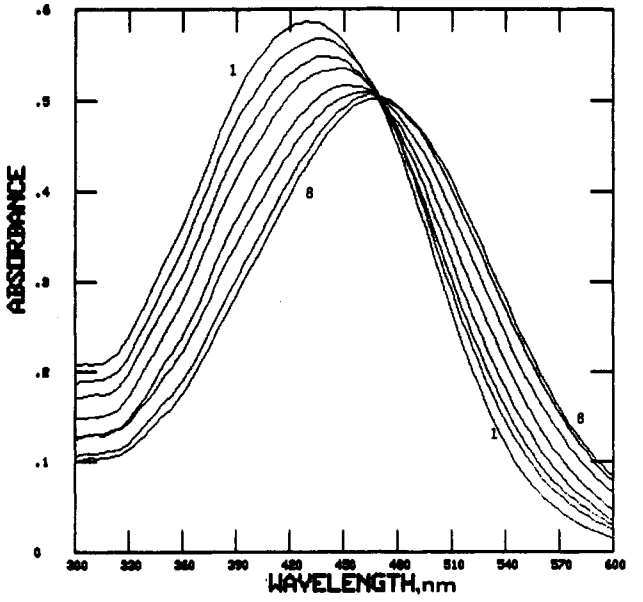

Figure 2. Equilibrium spectra for stage I for 136 μM ferrioxamine B (I = 2.0 M ($NaClO_4$); optical path length 1.72 cm): curve 1, starting spectrum of $Fe(HDFB)^+$, pH 6; curves 2–8, equilibria spectra for 0.02, 0.05, 0.10, 0.20, 0.40, 0.70, and 1.0 M $HClO_4$.

apparatus. In the hydrolysis experiments, $Fe(HDFB)^+$, usually 0.66 mM at pH ~6 and I = 2.0 M ($NaClO_4$), was mixed with $HClO_4/NaClO_4$ ($[H^+]$ = 0.04–2.0 M; I = 2.0 M). In some experiments $LiClO_4$ or NaCl was used as supporting electrolyte. In the formation experiments, the equilibrium mixture resulting from hydrolysis of $Fe(HDFB)^+$, 0.3 mM in 0.1 M H^+, was mixed with NaOH buffered with Hepes (final pH 7.4), acetic acid (final pH 3–4), or chloroacetic acid (pH ~3). The pseudo-first-order reaction of Fe^{3+} (68 μM) with $HDFB^+$ (0.5–5.0 mM) was examined at $[H^+]$ = 0.008, 0.08, and 0.8 M. Most of the kinetic experiments were monitored at 405, 426, or 471 nm, where there is a continuous decrease in absorbance during the hydrolysis. All reactions were studied at 25 ± 0.05 °C, I = 2.0 M usually maintained by $NaClO_4$. The computations of equilibria data were performed on a UNIVAC 1100 computer at the University Computer Center, Zagreb.

Results

Addition of solutions of $Fe(HDFB)^+$ at neutral pH to media of various acidities (>0.005 M H^+) results in different degrees of overall dissociation shown in eq 1, β_3 representing the overall

$$Fe(HDFB)^+ + 3H^+ \rightleftarrows Fe^{3+} + H_4DFB^+ \qquad \beta_3^{-1} \qquad (1)$$

formation constant, which is the usual way of expressing such equilibria. There is a shift in the absorbance maximum of the iron complex to higher wavelength during this process. At $[H^+] \geq 0.035$ M, four stages can be discerned. These are sufficiently different in their reaction times that they can be isolated from each other for spectral equilibria and kinetic analysis. For example, in 1.0 M $HClO_4$, the approximate half-lives for equilibrium to be reached for the four stages are 2 ms, 40 ms, 18 s, and 5 min; the resultant spectra at the end of each stage, when absorbance changes temporarily cease, are shown in Figure 1.[21] We refer to them as stages I–IV. Additional information on these processes could also be obtained by examining the reverse (formation) direction. Equilibria mixtures of ferrioxamine B in various degrees of hydrolysis ($[H^+] \geq 0.08$ M) were plunged into higher pH (≥3.0). This promoted complete formation of the hexadentate species, $Fe(HDFB)^+$, and the ring closures corresponding to the various stages could be separated and measured. The formation approach was particularly useful in examining stage IV, since the kinetics of hydrolysis were complex and not well-defined, whereas the reverse direction was rapid and kinetically simple.

Table I. Equilibria and Kinetic Parameters for the Various Stages in the Hydrolysis of Ferrioxamine B and in the Formation of Diferrioxamine B

n	k_n	k_{-n}	Q_n
1	(3.8 ± 0.3) × $10^{2\,a}$	(1.0 ± 0.1) × $10^{2\,b}$	3.7 ± 0.5[c,d]
		(0.8 ± 0.1) × $10^{2\,e}$	3.8 ± 0.3[c,f]
			3.6 (0.3)[c,d,g]
			5.2 (1.4)[c,f,g]
2	9.9 ± 0.9[b,e]	2.6 ± 0.1[b,e]	2.4 ± 0.2[d]
			3.9[f]
			2.1 (0.4);[d,g] >4.7[f,g]
3	(2.3 ± 0.2) × $10^{-2\,a}$	(1.7 ± 0.2) × $10^{-2\,b}$	2.0 ± 0.7[c,d]
			2.0 ± 0.3[c,f]
			3.4 (0.9)[c,d,g]
4	(5 ± 1) × $10^{-4\,a}$	2.0 ± 0.5[a]	(8 ± 3) × $10^{-5\,d}$
	0.65[h]	2.8 × $10^{2\,h}$	(2.4 ± 0.3) × $10^{-4\,f}$
			8 × $10^{-3\,d,g}$
5	(9.3 ± 0.5) × $10^{-4\,b}$	(3.6 ± 0.2) × $10^{3\,a}$	...
	0.016[h]	4.1 × $10^{3\,h}$	...
6	1.3 ± 0.4[a]	(2.6 ± 0.3) × $10^{-3\,a}$	(5.2 ± 0.8) × $10^{2\,d}$
	52[h]	0.91[h]	57[d,h]
7	(1.6 ± 0.1) × $10^{3\,a}$	(3.5 ± 0.5) × $10^{-3\,b}$	
	3.5 × $10^{3\,h}$	0.105[h]	

[a] M^{-1} s^{-1}. [b] s^{-1}. [c] M^{-1}. [d] Spectral analysis. [e] Data from formation direction. [f] Calculation from kinetic data. [g] Reference 11; value in parentheses is uncertainty—standard deviation of parameters obtained from a nonlinear least-squares analysis using theoretical equations. [h] I = 1.0 M (NaCl); ref 13.

Stage I. Figure 2 shows a set of spectra obtained at the end of stage I in various acidities (0.02–1.0 M H^+). Each spectrum was collected when spectral changes temporarily ceased, about 5 half-lives for equilibration, at which time stage I was almost complete and stage II had just commenced (~5–10%). There was a clean isosbestic point at 471 nm. For the equilibrium

$$Fe(HDFB)^+ + H^+ \rightleftarrows Fe(H_2DFB)^{2+} \qquad k_1, k_{-1}, Q_1 \qquad (2)$$

it is easily shown that the absorbance at any wavelength, at equilibrium for stage I, A^I, should obey the expression

$$A^I = \frac{\epsilon_{Fe(HDFB)^+} + \epsilon_{Fe(H_2DFB)^{2+}} Q_1[H^+]}{1 + Q_1[H^+]} \times ([Fe(HDFB)^+] + [Fe(H_2DFB)^{2+}]) \qquad (3)$$

(21) The dead time of our instrument is 3–4 ms. The spectrum is recorded immediately after mixing with a scan time of 3.8 ms, scanning from lower to higher wavelengths. This means that the peak portions of the spectra are recorded about 5–6 ms after reaction initiation. Thus, in the recording of curve 2 in Figure 1, part (~10–15%) of stage II has occurred. The fortunate similarity of the spectra at the end of stages I and II means however that spectrum 2 shown is close to that for the end of stage I, before intervention of stage II.

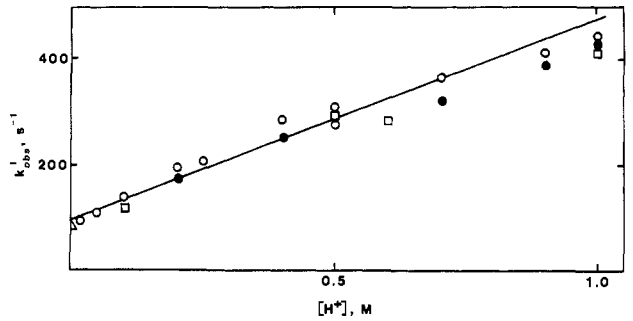

Figure 3. Observed first-order rate constant for stage I (k^{I}_{obsd}) as a function of $[H^+]$: (○) $NaClO_4$; (□) $LiClO_4$; (●) NaCl; (△) pH drop to lower acidity, $NaClO_4$. Line was calculated for eq 4. In all conditions, 330 μM ferrioxamine B was used and I = 2.0 M.

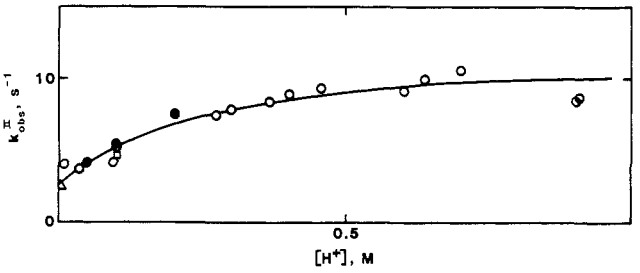

Figure 4. Observed first-order rate constant for stage II (k^{II}_{obsd}) as a function of $[H^+]$: (○) $NaClO_4$; (□) $LiClO_4$; (●) NaCl; (△) pH drop to lower acidity, $NaClO_4$. Line was calculated for eq 8. In all conditions, 330 μM ferrioxamine B was used, I = 2.0 M, and λ = 426 nm.

Analysis of A^{I} at 375, 405, and 426 nm was consistent with (3), leading to a Q_1 value shown in Table I.

The approach to equilibrium in stage I is first order. The associated rate constant (k^{I}_{obsd}) is related to $[H^+]$ by (4), shown in Figure 3. Within a fairly large experimental error (arising from the very fast reactions), the values of k^{I}_{obsd} were unaffected by a change of supporting electrolyte from $NaClO_4$ to $LiClO_4$ or NaCl (Figure 3). The values of k^{I}_{obsd} were also unchanged by the presence of either excess H_4DFB^+ or $Fe(ClO_4)_3$ in the reacting solutions. The values of k_1 and k_{-1} are shown in Table I. The value of k_{-1} could also be determined directly by formation studies referred to above (Table I).

$$k^{I}_{obsd} = k_1[H^+] + k_{-1} \quad (4)$$

Stage II. At the end of the second stage of hydrolysis, a preliminary assumption is made that, in addition to the species involved in stage I, there is present a third species Fe* related to $Fe(H_2DFB)^{2+}$ by

$$Fe(H_2DFB)^{2+} + nH^+ \rightleftarrows Fe^* \qquad Q_2 \quad (5)$$

The absorbance at the end of stage II, A^{II}, is given by

$$A^{II} = \frac{\epsilon_a + \epsilon_b Q_1[H^+] + \epsilon_c Q_1 Q_2 [H^+]^{n+1}}{1 + Q_1[H^+] + Q_1Q_2[H^+]^{n+1}}([a] + [b] + [c]) \quad (6)$$

where a, b, and c are the species $Fe(HDFB)^+$, $Fe(H_2DFB)^{2+}$, and $Fe(H_2DFB)^{2+*}$. A nonlinear least-squares analysis of the spectrophotometric data led to values of n = 0.09 ± 0.01 (375 nm) and n = 0.07 ± 0.01 (405 nm). It is clear then that no protons are involved in stage II. The value of Q_2 was reevaluated from the data with the assumption that n = 0. The species Fe* is thus a different form of $Fe(H_2DFB)^{2+}$, designated $Fe(H_2DFB)^{2+*}$, and the equilibrium for stage II is as shown in (7). The approach to equilibrium in stage II is nicely first order, with no difficulties in assessing the final equilibrium values. The $k^{II}_{obsd}/[H^+]$ profile is displayed in Figure 4. It is consistent with expression 8, which

$$Fe(H_2DFB)^{2+} \rightleftarrows Fe(H_2DFB)^{2+*} \qquad k_2, k_{-2}, Q_2 \quad (7)$$

$$k^{II}_{obsd} = \frac{k_2 Q_1 [H^+]}{1 + Q_1[H^+]} + k_{-2} \quad (8)$$

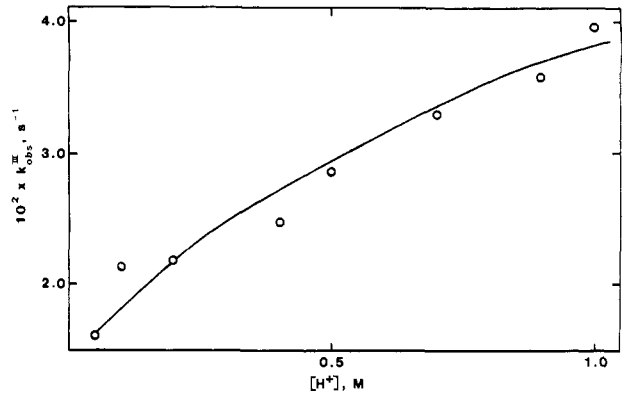

Figure 5. Observed first-order rate constant for stage III (k^{III}_{obsd}) as a function of $[H^+]$. In all conditions, 330 μM ferrioxamine B was used and I = 2.0 M ($NaClO_4$).

is expected for the combination of reaction 2 with reaction 7. The value of k_{-2} (2.6 s^{-1}) was accurately assessed by formation measurements at pH 3–4. The calculated line in Figure 4 results from values of k_2, k_{-2}, and Q_1 shown in Table I. The rates were unaffected by changing the reaction medium (Figure 4). However at $[H^+] \geq 0.5$ M, the rate constants measured at 540 nm were larger than those at 426 nm, and we are at a loss to explain this.

Stage III. Combination of reactions 2 and 7 with

$$Fe(H_2DFB)^{2+*} + H^+ \rightleftarrows Fe(H_3DFB)^{3+} \qquad k_3, k_{-3}, Q_3 \quad (9)$$

yields eq 10 for the dependence of the absorbance after stage III,

$$A^{III} = \frac{\epsilon_a + \epsilon_b Q_1[H^+] + \epsilon_c Q_1Q_2[H^+] + \epsilon_d Q_1Q_2Q_3[H^+]^2}{1 + Q_1[H^+] + Q_1Q_2[H^+] + Q_1Q_2Q_3[H^+]^2} \times ([a] + [b] + [c] + [d]) \quad (10)$$

A^{III}, on the hydrogen ion concentration. a, b, and c, are the species defined in (6), and d is $Fe(H_3DFB)^{3+}$. A nonlinear least-squares fit of A^{III} values, obtained at 426 nm and various $[H^+]$'s with values for the parameters already obtained, yields a value for Q_3 (Table I).

Good kinetic data for stage III of the hydrolysis were the most difficult to obtain of any stage. The reaction was at least 2 orders of magnitude slower than the previous stage, and kinetic separation from this was easy. However, it was difficult to separate the completion of stage III and the incidence of stage IV. In the *estimation* of this lies most of the error in measuring k^{III}_{obsd}, the first-order rate constant for attainment of equilibrium for this stage. On the basis of a scheme involving preequilibria 2 and 7 and a rate-determining equilibration toward $Fe(H_3DFB)^{3+}$ via (11), an equation (12) is derived. The best fit of the data to eq

$$\begin{array}{ccc} Fe(H_2DFB)^{2+} & & \\ \uparrow\downarrow & \overset{k_3(H^+)}{\underset{k_{-3}}{\rightleftharpoons}} & Fe(H_2DFB)^{3+} \\ Fe(H_2DFB)^{2+*} & & \end{array} \quad (11)$$

$$k^{III}_{obsd} = k_3 \frac{Q_1(1 + Q_2)[H^+]^2}{1 + Q_1(1 + Q_2)[H^+]} + \frac{1 + Q_2^{-1}}{Q_3} \quad (12)$$

12 (Figure 5) yields the values of k_3 and Q_3 collected in Table I. The third stage was *not* observed (although stages I and II were unchanged) when hydrolysis was carried out in the presence of H_4DFB^+ (0.01–1.0 mM, 0.04–0.90 M $HClO_4$) in excess over ferrioxamine B (0.05–0.22 mM).

Stage IV. The dependence of the *final* equilibrium absorbance A^{IV} on the H^+ concentration is based on a scheme comprising reactions 2, 7, 9, and 13 and assumes a total proton change of

$$Fe(H_3DFB)^{3+} + H^+ \rightleftarrows Fe^{3+} + H_4DFB^+ \qquad Q_4 \quad (13)$$

3. It is expressed by eq 14–17. The ε's refer to a = $Fe(HDFB)^+$,

$$A^{IV} = \frac{2Gc_tP + GN^2 \pm GN(4c_tP + N^2)^{1/2}}{2P^2} \quad (14)$$

$$G = \epsilon_a + \epsilon_bQ_1[H^+] + \epsilon_cQ_1Q_2[H^+] + \epsilon_dQ_1Q_2Q_3[H^+]^2 \quad (15)$$

$$P = 1 + Q_1[H^+] + Q_1Q_2[H^+] + Q_1Q_2Q_3[H^+]^2 \quad (16)$$

$$N = (Q_1Q_2Q_3Q_4[H^+]^3)^{1/2} \quad (17)$$

b = $Fe(H_2DFB)^{2+}$, c = $Fe(H_2DFB)^{2+*}$, and d = $Fe(H_3DFB)^{3+}$ at 426 nm, obtained from the previous stages, and are respectively 2403 (20), 1597 (17), 1415 (40) and 1221 (76) M^{-1} cm^{-1}. The absorbance of the product species, Fe^{3+} and H_4DFB^+, is assumed zero in the wavelength range studied and c_t represents the sum of the concentrations of $Fe(HDFB)^+$, $Fe(H_2DFB)^{2+}$, $Fe(H_2DFB)^{2+*}$, $Fe(H_3DFB)^{3+}$, and Fe^{3+}. The fitting of eq 14 to A^{IV} data and equilibria parameters, already determined from previous stages, yields a value for Q_4 shown in Table I. A real value of Q_4 was obtained only by using a negative sign in eq 14.

The rate of hydrolysis for stage IV is more than 10 times slower than that of the third stage. We were not able, however, to fit satisfactorily the observed first-order rate constants for this equilibration k^{IV}_{obsd} to the derived equations (18) and (19)[22] for a scheme involving preequilibria (stages I–III), followed by the rate-determining steps (20) and (21). Therefore, a series of

$$k^{IV}_{obsd} = (k_{-4} + k_{-5}K_h[H^+]^{-1})([H_4DFB^+]_e + [Fe(III)]_e) + (k_4[H^+] + k_5)A \quad (18)$$

$$A = \frac{Q_1Q_2Q_3[H^+]^2}{1 + Q_1[H^+] + Q_1Q_2[H^+] + Q_1Q_2Q_3[H^+]^2} \quad (19)$$

$$Fe(H_3DFB)^{3+} + H^+ \rightleftarrows Fe^{3+} + H_4DFB^+ \qquad k_4, k_{-4} \quad (20)$$

$$Fe(H_3DFB)^{3+} \rightleftarrows FeOH^{2+} + H_4DFB^+ \qquad k_5, k_{-5} \quad (21)$$

$$Fe^{3+} \rightleftarrows FeOH + H^+ \qquad K_h = 1.1 \times 10^{-3}\ M \quad (22)$$

experiments were undertaken in which the interaction of iron(III) with excess H_4DFB^+ (i.e. the reverse of reactions 20 and 21) was measured. The concentrations of H_4DFB^+ that were used were such as to ensure pseudo-first-order conditions, as well as effect complete removal of ferric ion. The spectrum of the product was identical with that of ferrioxamine B even with a large excess of H_4DFB^+. The formation of $Fe(H_3DFB)^{3+}$ was observed as a uniphasic first-order absorbance change at 500 nm. At other wavelengths, the subsequent slower formation of $Fe(HDFB)^+$ could be observed controlled by the back-reaction of stage II (k_{-2}). There was no sign of the very slow stage III (k_{-3}). These observations were made by rapid scan. The pseudo-first-order formation rate constant k^{-IV}_{obsd} is given by (23). The plot of

$$k^{-IV}_{obsd} = (k_{-4}[H^+] + k_{-5}K_h)([H^+] + K_h)^{-1}[H_4DFB^+] \quad (23)$$

k^{-IV}_{obsd} vs. $[H_4DFB^+]$ was linear (Figure 6). The values of k_{-4} and k_{-5} (Table I) were obtained by fitting the experimental data to eq 23. Combining these values with the kinetic hydrolysis data and (18)[22] allowed computation of the k_4, k_5, and Q_4 values listed in Table I. The best fit of all data yields a $k_{obsd}/[H^+]$ profile for hydrolysis shown in Figure 6 (inset), which also shows the Monzyk and Crumbliss[11] experimental data.

Dimer Formation. $Fe(HDFB)^+$ reacts with excess ferric ion in acid solution to give the dimer $Fe_2(HDFB)^{4+}$ ion.[12,14,17,18] Figure 7 shows the results of a rapid-scan, stopped-flow examination of the system. The first stage of hydrolysis of $Fe(HDFB)^+$ is clearly seen, and this is followed by interaction of the fragment with the iron(III) ion. Using the approach detailed previously,[14] the kinetic scheme comprising reactions 24 and 25 in addition to reaction

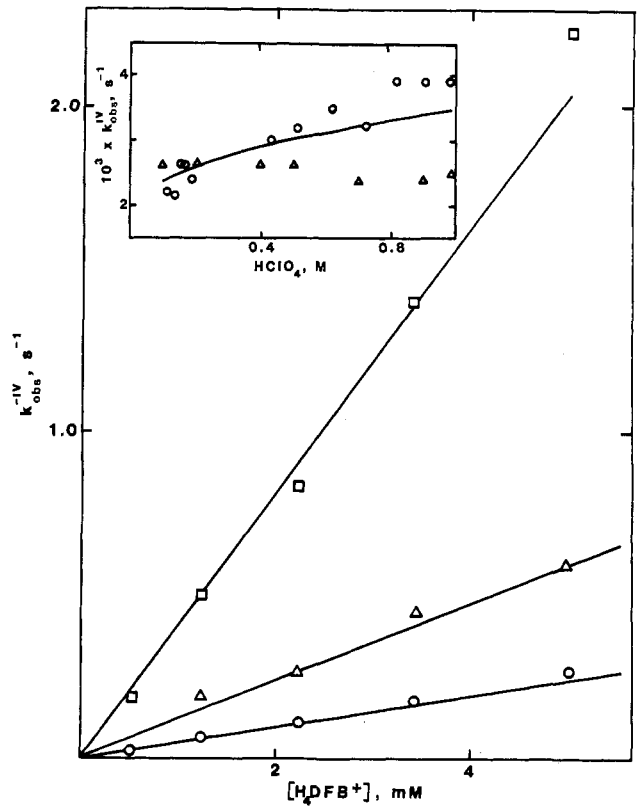

Figure 6. Observed first-order rate constant for formation of $Fe(H_3DFB)^{3+}$ (k^{-IV}_{obsd}) as a function of $[HDFB^+]$: (□) $[H^+]$ = 0.008 M; (○) $[H^+]$ = 0.08 M; (△) $[H^+]$ = 0.8 M (ordinate should be divided by 20 for this entry). $[Fe(ClO_4)_3]$ = 68 μM. Inset: dependence of observed first-order rate constant for stage IV (k^{IV}_{obsd}) as a function of $[H^+]$: (△) our data; (○) data of ref 11. Line was calculated for eq 18. In all conditions, 330 μM ferrioxamine B was used and I = 2.0 M.

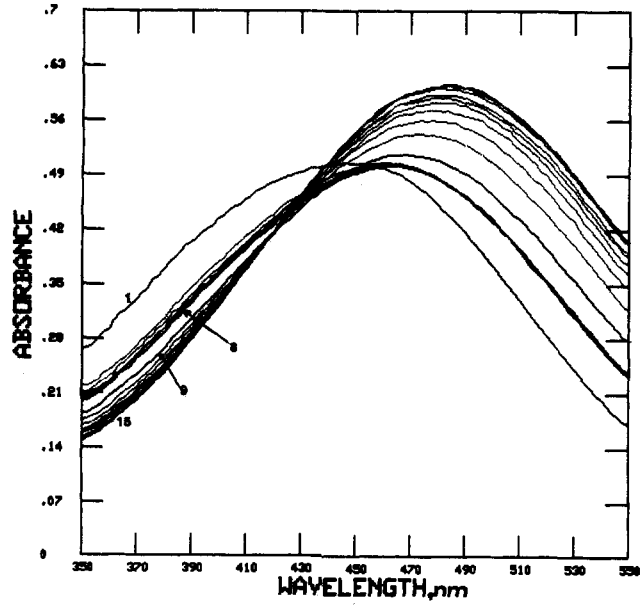

Figure 7. Rapid scan for reaction of ferrioxamine B (0.11 mM) with $Fe(ClO_4)_3$ (1.16 mM) in 0.1 M H^+ (I = 2.0 M ($NaClO_4$)): spectrum 1, recorded 3.8 ms after mixing;[21] spectra 2–8, recorded at 0.286-s intervals after spectrum 1, so that spectrum 8 was recorded 2 s after mixing; spectra 9–14, recorded 11.4, 22.8, 34.2, 45.6, 57.0, and 68.4 s after mixing; spectrum 15, recorded 160 s after mixing. These spectra result from three separate experiments; optical path length 1.72 cm. Dimer formation is ~80% complete under these conditions.

(22) The calculation of the equilibrium concentrations $[H_4DFB^+]_e$ and $[Fe(III)]_e$ in eq 18 was made by using a subroutine based on the Newton–Raphson iterative method, as a segment of the main program (Sharma, V. S.; Leussing, D. L. *Talanta* **1971**, *18*, 1137) employed in modified version for simultaneous refining of the constant k_{-1}/k_1 and for all data-reduction analysis.

(23) Milburn, R. M.; Vosburgh, W. C. *J. Am. Chem. Soc.* **1955**, *77*, 1352.

$$Fe(H_2DFB)^{2+} + Fe^{3+} \rightleftarrows Fe_2(HDFB)^{4+} + H^+ \quad (24)$$
$$k_6, k_{-6}, Q_6$$

$$Fe(H_2DFB)^{2+} + FeOH^{2+} \rightleftarrows Fe_2(HDFB)^{4+} \quad k_7, k_{-7} \quad (25)$$

22 explains well the kinetic data. The results are collected in Table I and are compared with previous results in a 1.0 M ionic strength medium comprising NaCl.[14]

The interchange of metal ions in (26) was also briefly studied by rapid-scan stopped flow. No attempt at a kinetic analysis was

$$Al(HDFB)^+ + Fe^{3+} \rightleftarrows Fe(HDFB)^+ + Al^{3+} \quad (26)$$

made. A neutral solution containing $Al(HDFB)^+$ (11 mM, I = 2.0 M ($NaClO_4$)) was mixed with $Fe(ClO_4)_3$ (0.44 mM, 8 mM $HClO_4$, I = 2.0 M ($NaClO_4$)). The first spectrum (3.8 ms) exhibited a maximum at ~485 nm, and subsequent spectra showed a continuous shift of the maximum to shorter wavelengths, with an isobestic point at ~470 nm preceding the final formation of $Fe(HDFB)^+$. The whole process occupied about 80 s.

Discussion

In the work reported here, there is qualitative and often quantitative agreement with a number of the observations made by Monzyk and Crumbliss[11] on the hydrolysis of $Fe(HDFB)^+$ under the same conditions, namely acid perchlorate (I = 2.0 M) and 25 °C. Four separable equilibria, in similar time ranges, were confirmed (eq 27). There is a shift in the absorbance maximum

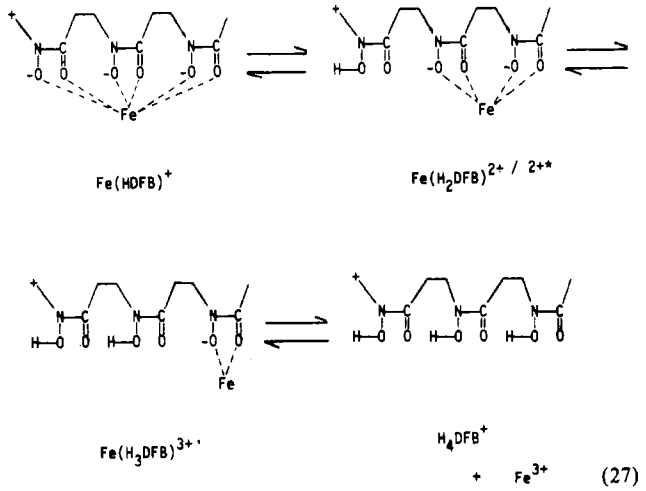

(27)

toward longer wavelengths and lowered intensity[11] (Figure 1). Even in 1 M H^+ at equilibrium all species shown in (27) are present, even if $Fe(HDFB)^+$ and $Fe(H_2DFB)^{2+}$ are in small amounts.[24] There are, however, important differences in the results of the two investigations both in the data obtained and in their manipulation, more particularly in the kinetic aspects (Table I). With such a large range of proton concentration examined, even with a constant ionic strength, we deemed it important to change the supporting electrolyte (from $NaClO_4$ to $LiClO_4$).[25] No marked differences in the characteristics of the four stages were observed when this substitution was made (Figures 3 and 4). Each stage will now be discussed. They correspond to those designated very fast, fast, slow, and very slow by previous workers.[11]

Stage I. The spectra at the end of stage I in various acidities were obtained by rapid-scan spectrophotometry (Figure 2). The isosbestic point indicates that only two species are of major importance in this stage. From absorbance data at a number of wavelengths, the equilibrium associated with this stage can be shown to be proton-dependent and the equilibrium constant for (2), Q_1, can be easily calculated. This value is in excellent agreement with that reported[11] (Table I) and in fair agreement with that measured by Schwarzenbach and Schwarzenbach (8.8 M^{-1} at 20 °C and I = 0.1 M; see also footnote 36 in ref 11). The high rate associated with this equilibration is undoubtedly the cause of differing assignments of rate law. Previous work[11] indicated a H^+-independent first-order rate constant ~300 s^{-1}, whereas our data show a direct dependence of the rate of hydrolysis on $[H^+]$ (Figure 3). Evidence for the correctness of our data is twofold. The value of Q_1 obtained from the rate constants is in very good agreement with that deduced spectrally (Table I). Secondly, the rate law (4) can be confirmed by experiments at lowered temperature (6 °C), where the slower rates are more easily measured accurately.[26]

Undoubtedly the product of this stage, $Fe(H_2DFB)^{2+}$, is the easiest of the three intermediates to characterize. It is considered to be the fragment resulting from partial unwrapping of the fully attached ligand in $Fe(HDFB)^+$, beginning at the protonated amine end of the molecule shown schematically in eq 27.[11] The spectral peak and molar absorbance coefficients for $Fe(H_2DFB)^{2+}$ (ϵ_{480nm} = 2.15 × 10^3 M^{-1} cm^{-1}) almost coincide with those for the bis(acetohydroxamato)iron(III) ion (ϵ_{470nm} = 2.0 × 10^3 M^{-1} cm^{-1}).[19] The parameters in Table I associated with this stage may be compared with those for the comparable change (28) involving

$$Fe(CH_3CONHO)_3 + H^+ + 2H_2O \rightleftarrows Fe(CH_3CONHO)_2(H_2O)_2^+ + CH_3C(O)NHOH \quad (28)$$

conversion of the tris- into the bis(acetohydroxamato)iron(III) complex.[19] The proton-assisted removal of one acetohydroxamate residue in (28) is much easier (k = 1.0 × 10^5 M^{-1} s^{-1}) than for loosening the same moiety in ferrioxamine B (3.8 × 10^2 M^{-1} s^{-1}). This may reflect a hydrophobic environment in the latter (preventing easy access of hydrated proton) being more important than strain considerations, which are likely to be higher in the hexacoordinated ligand (and leading to easier breakage).

This stage was missed in previous studies of ferrioxamine B in which the first ring opening was an integral feature. These include acid hydrolysis investigations, where a stopped-flow apparatus with dead time about 10 ms was used,[13] and ligand-interchange experiments involving initial rate experiments with conventional monitoring.[15]

Stage II. A small, but definite, spectral change is associated with this stage (Figure 1). Analysis of equilibria spectra shows that no protons are involved, indicating that there is no permanent further Fe–O bond breakage in (7). The agreement with previous workers'[11] estimates of Q_2 (2.1) is excellent and of k_2 (14 s^{-1}) and k_{-2} (<3 s^{-1}) is fair. Our determination of k_{-2} directly from the opposite direction is unequivocal. The value of Q_2 obtained by kinetics (3.9 or > 4.7[11]) is in poor agreement with that obtained by spectral analysis and we cannot explain this, although small absorbance changes may contribute to measurement errors. The identification of $Fe(H_2DFB)^{2+*}$ is speculative, and we have ommited its structure in (27). The dissociating hydroxamate oxygen atom may be hydrogen bonded to adjacent coordinated water on the iron (a type of three-coordinated ligand),[11] or some rearrangement of the four-coordinated ligand about the iron (cis → trans?) may be involved.

Stage III. The differences between values of Q_3 determined in this and in previous work[11] are small, given the experimental errors involved (Table I). The kinetics are consistent with a H^+-assisted breakage of a hydroxamate residue in the $Fe(H_2DFB)^{2+}/Fe(H_2DFB)^{2+*}$ reactant mixtures. The experimental data are in good agreement with the derived kinetic expression (12) (Figure 5). This stage was treated by Monzyk and Crumbliss[11] as a rapid $[H^+]$-preequilibrium process for which K^1k_4 = (<0.4 M^{-1})(1.8 × 10^{-1} s^{-1}) ≤ 7.2 × 10^{-2} M^{-1} s^{-1}; on the basis of our k_3 (=2.3 × 10^{-2} M^{-1} s^{-1}) the values appear to be consistent. The proton-assisted removal of the second hydroxamate residue invoked in this stage is 5 orders of magnitude slower than that for the conversion of a bis(acetohydroxamato)- to a mono(acetohydroxamato)iron(III) complex (1.4 × 10^3 M^{-1} s^{-1} at I = 2.0

(24) In 1.0 M H^+ at equilibrium, there is less than 3% of $Fe(HDFB)^+$ present, but in 0.1 M H^+ this value reaches about 40%.

(25) Wilkins, R. G. *The Study of Kinetics and Mechanism of Reactions of Transition Metal Complexes*; Allyn and Bacon: Boston, MA, 1974.

(26) Krznarič, G. Master's Thesis; University of Zagreb, 1985; unpublished observations.

M and 25 °C[19]). It is reasonable to suppose that the product of this stage, $Fe(H_3DFB)^{3+}$, contains only one coordinated hydroxamate residue and that this is a terminal one; see (27). The computed spectrum of this species on the basis of Figure 1 and the known Q values has a maximum at ~480 nm. Although admittedly approximate, this is nearer that of bis(acetohydroxamato)iron(III) (470 nm) than that of the mono complex (505 nm). However, the uncoordinated attached portion may modify the maximum position, since the maximum is shifted to 480 nm for mono(betainehydroxamato)iron(III), $Fe(RCONHO)(H_2O)_4^{2+}$, R = $(CH_3)_3N^+-CH_2$.[27] In an attempt to satisfy ourselves further on this point, we studied, briefly by rapid scan, the reaction (26). We reasoned that the expected slow and stepwise stripping of the ligand from the colorless aluminum complex *might* give as a first intermediate a species in which the aluminum is attached to four donors and the iron is attached to two donors of the desferral. Although the iron binding site would probably be at the opposite end of the trihydroxamate chain compared with that in ferrioxamine B hydrolysis, this mixed species should resemble spectrally that of $Fe(H_3DFB)^{3+}$. The maximum position was, satisfying, at ~485 nm.

Stage IV. The last stage leads to ferric ion and the free tetraprotonated ligand (reaction 13). The computed value of Q_4 from spectral analysis of the final equilibrium mixture is markedly smaller than previously assessed[11] (Table I), where stage I was eliminated from consideration since positive equilibrium constants could only then be obtained.[11,24] We can now compute the overall stability constant β_3 in (1) using the Q's of each stage, since $\beta_3 = (Q_1Q_2Q_3Q_4)^{-1}$. The value, 7.0×10^2 M^2, is in good agreement with those determined spectrally,[8] 1.0×10^3 M^2 [26] and 3.0×10^3 M^2 (20 °C, I = 0.1 M[8]). The value computed from Monzyk and Crumbliss' data[11] is 4.9 M^2. Our fuller treatment appears justified. The smaller value of Q_4 (2.4×10^{-4}) for hydrolysis of $Fe(H_3DFB)^{3+}$ compared to that for hydrolysis of $Fe(CH_3CONHO)(H_2O)_4^+$ ($Q_3 = 10^{-2}$ [19]) is surprising. The kinetics for this stage were best investigated from the formation direction, since these were simpler to interpret with lesser suppositions than for the hydrolysis (compare (18) and (19) with (23)). The formation of $Fe(H_3DFB)^{3+}$, using excess ligand over iron(III), was nicely first order at 500 nm. Further ring closures did not interfere at this observation wavelength but could be observed, for example, at 570 nm. Interestingly, these further changes were controlled by stage 2 (k_{-2}) followed by very rapid complete conversion to $Fe(HDFB)^+$. The apparent absence of the slow third stage we suppose arises from its acceleration by free ligand perhaps via a labile iron-bridged diligand species which has been invoked as an active intermediate in other studies.[10] It is significant that the third stage is also not observed during the hydrolysis of ferrioxamine B in the presence of free ligand. The linear dependence of k_{obsd} on the concentration of H_4DFB^+, in excess (Figure 6), is strong support for the notion that the first stage of chelation was being measured. The second-order formation has been previously observed in a formate medium.[10] The second-order rate constants for formation of $Fe(H_3DFB)^{3+}$ from Fe^{3+} and $FeOH^{2+}$ (Table I) are close to the corresponding values for the formation of $Fe(CH_3CONHO)(H_2O)_4^+$ (4.8 and 4.1×10^3 M^{-1} s^{-1}, respectively). We can utilize the formation rate constants and hydrolytic equilibria data from (14)–(17) to calculate the rate data for hydrolysis (Table I) and compute the expected variation of $k^{IV}_{obsd}/[H^+]$ from (18). As Figure 6 (inset) shows, a very small increase of k^{IV}_{obsd} with $[H^+]$ would be anticipated. Our data do not show this (hence our problems with fitting kinetic data to (18)), although Monzyk and Crumbliss' data[11] are in better agreement. We do not understand this, but one should note the number of parameters that must be used to solve (18).

Dimer Formation. Rapid scan of the iron(III)–ferrioxamine B reaction in acid solution shows that the early stages of hydrolysis precedes the formation of the dimer (Figure 7). Spectra 1–8 correspond to equilibration of stages I and II. The protonated forms $Fe(H_2DFB)^{2+}$ and $Fe(H_2DFB)^{2+*}$ are thus active participants. It is interesting to note that the rate constants for reaction of $Fe(H_2DFB)^{2+}$ and H_4DFB^+ with Fe^{3+} are similar (1.3 and 2.0 s^{-1}, respectively) and that the corresponding reactions with $FeOH^{2+}$ are both about 10^3 times faster, which is a common behavior with iron(III)–ligand interaction.[7,25] The rate constants for hydrolyses of $Fe(H_3DFB)^{3+}$ to Fe^{3+} or $FeOH^{2+}$(4.9×10^{-4} M^{-1} s^{-1} and 9.3×10^{-4} s^{-1}, respectively) are also close to those for the corresponding hydrolysis of $Fe_2(HDFB)^{4+}$, i.e. 2.6×10^{-3} M^{-1} s^{-1} and 3.5×10^{-3} s^{-1}, respectively. Comparison with previous results shows that chloride ion labilizes both reactions of $Fe(H_2DFB)^{2+}$ and H_4DFB^+ with iron(III), because of the greater reactivity of the iron(III)–chloro species (see Table I).[14,26]

In conclusion, the four stages in the acid hydrolysis of ferrioxamine B previously observed[11] have been confirmed in this study. The only significant difference in the equilibrium results of the two studies is in stage IV, but there is some disagreement in the kinetic results both in the observed rate constants and in the nature of the rate laws. In stage I, we observe a $[H^+]$ dependence whereas Monzyk and Crumbliss[11] do not, although the extreme rapidity may contribute to this disagreement. We could not detect a proton dependence on the aquation rate of stage IV, although it was expected on the basis of the mechanism we proposed from the results of the reverse direction (formation). The aquation rate dependence on $[H^+]$ for stage IV observed by Monzyk and Crumbliss[11] is however in better agreement with our kinetic analysis! Some slight differences in rates for stage III are noted, although we had difficulties in analyzing this stage. There is thus a good deal of satisfying agreement between the two studies. Some puzzles remain and the resolution of these will require other approaches, for example, different monitoring methods or examination of schizokinen, which contains only two hydroxametic residues. Although the behavior of ferrioxamine B in high acid is biologically irrelevant, the mechanism of dechelation forms a basis for understanding the unwrapping process in neutral or weakly acid media, interchange processes, and catalyzed hydrolyses. This is important in the mechanism of iron binding and release by the clinically important siderophore.

Acknowledgment. This work received financial support from the National Science Foundation, the Croatian Council for Research, and the National Institutes of Health through the U. S.-Yugoslav Joint Board on Scientific and Technological Cooperation. These are gratefully acknowledged. Desferrioxamine B was from Ciba-Geigy, and we thank them for this gift. We appreciate very helpful comments on the manuscript by Drs. A. L. Crumbliss and D. W. Margerum.

(27) Biruš, M.; Kujundžič, N.; Pribanič, M.; Tabor, Z. *Croat. Chem. Acta* **1984**, *57*, 313.